p-ISSN 2301–4156 | e-ISSN 2460–5719

DC Microgrid Performance Improvement Strategy with DC/AC Coupling Configuration

Adhi Kusmantoro[1], Ardyono Priyadi[2]

[1] Department of Electrical Engineering, Universitas PGRI Semarang, Semarang 50232 INDONESIA, (tel.: 024-831 6377; fax: 024-8448217, email: adhikusmantoro@upgris.ac.id
[2] Department of Electrical Engineering Faculty of Intelligent Electrical and Informatics Technology Institut Teknologi Sepuluh Nopember, Surabaya 60117 INDONESIA (tel.: 031-5947274; fax: 031-5923465; email: priyadi@ee.its.ac.id)

[Received: 11 April 2023, Revised: 26 June 2023]
Corresponding Author: Adhi Kusmantoro

ABSTRACT — DC microgrid is a good solution for increasing demand for electricity loads and is an effective way to utilize renewable energy sources into distributed generation systems. Solar energy has intermittent properties when DC microgrids are used. In the previous research, the battery was used as an energy reserve to overcome fluctuations in the output power of photovoltaic (PV) arrays. However, the use of many batteries requires a high cost. This study aims to reduce power fluctuations on the DC bus, when the DC microgrid source from the PV array and battery is disconnected. The research method was carried out using MATLAB simulations, by designing a DC/AC coupling hybrid configuration. This configuration used two PV arrays, two multi-battery sources, and a utility network. DC microgrid settings were done separately by each converter by sending a reference signal to the converter control. In the first condition, the DC load and AC load were supplied from the PV array. In the second condition, the load was supplied from the battery. Meanwhile, in the third condition, the load was supplied from the utility network. The results showed that when using a PV array source, the DC bus voltage remained stable at 48 V, even though there was a spike at 08.00 and 15.00. Likewise, when using a battery source and utility network, the DC bus voltage was maintained at a level of 48 V. In this study, the DC microgrid was able to supply the load uninterruptedly using three conditions or modes. Therefore, the DC microgrid hybrid configuration can provide continuous electric power.

KEYWORDS — Microgrid, Battery, PV, Converter, MPPT.

I. INTRODUCTION

With the increase in population and technological developments, the demand for electricity sources has increased significantly, but large power plants are still using fossil fuels which are becoming increasingly depleting. Indonesia is a country with abundant sources of renewable energy, especially the potential for solar energy as a source of microgrids. DC microgrid has many advantages when compared to AC microgrid, so it gets a lot of attention for development [1].

Microgrid operates by integrating many new renewable energy sources, for example solar energy, wind, biodiesel. The integration of the renewable sources will continue to raise every year, thereby affecting the availability of load power sources. In the future, all sources of electricity will be obtained from renewable energy [2], [3]. DC microgrid can operate independently and not connected to the utility network. This method is widely implemented in areas that are not covered by electricity utility. Nevertheless, an optimal control strategy is necessitated for the DC-DC converter to improve the performance of the DC microgrid since DC microgrid has many converters connected in parallel to supply the load [4].

Although there is numerous renewable energy available, solar and wind energy are the energy that is frequently used as a microgrid source. However, these energies have an intermittent nature, so an energy storage according to the load capacity system is needed [5]. In utilizing solar energy as a source of electricity, photovoltaic (PV) is used. There are many factors that influence the use of PV to obtain maximum output power. The influencing factors involve the position of the PV to the sun and the ambient temperature. One of the methods to increase PV output is to adjust the position of PV precisely to the sun using a solar tracker. Using solar tracker, the PV position can be adjusted following the sun, so that the intensity of solar irradiation will reach geometric points [6], [7]. This solar tracker will set tracking at the point of maximum power, according to the PV curve used. With this method, the PV efficiency will increase. The performance of this method depends on the quality and ability of the sensor to detect the sun accurately, as well as the availability of energy in the PV driving motor. Besides, this method is only suitable for use when the weather is sunny [8].

DC microgrid uses DC-DC converters to regulate the flow of energy from renewable energy sources to load and energy storage. DC microgrid usually uses a converter with a single input. Many input converters with centralized control can be used to improve DC microgrid performance [9]. When the microgrid uses the PV without an energy storage, the energy supply to the load will be cut off even when a solar tracker is used to produce maximum output power. Therefore, it is very necessary to store energy to supply the load at night or when intermittent PV occurs. The battery storage method can be used to store PV energy. Battery storage uses a bidirectional DC-DC converter for the charging and discharging process. The weakness of this method is that it requires a large battery at a high price [10]. The linearization method is used in the DC-DC converter to improve the efficiency of power distribution to the load. Linearization modeling is done on the converter connected to the PV. With this method, there is an increase in the output power to the load. This method is used in boost converters [11]–[13].

Another method is carried out by designing a four-phase interleaved DC-DC converter, with a single ended primary converter (SEPIC)-Cuk converter combination. Converter design is done for single input multi-output (SIMO). By incorporating a converter, a corresponding increase in voltage is obtained to the DC bus. The interleaved converter method can improve the DC microgrid performance so that it has better

p-ISSN 2301–4156 | e-ISSN 2460–5719

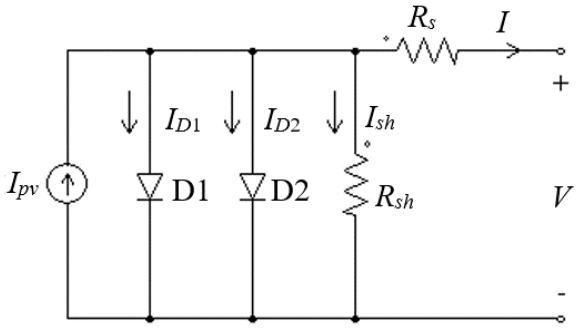

Figure 1. PV model with R_s and R_{sh}.

system response and increasing efficiency. The weakness of the system used is its greater power loss due to the use of more converters [14], [15]. Multiple input Cuk converters are used with soft switching settings to increase the efficiency of the DC-DC converter. This method will improve the stability of the DC bus voltage. When one of the output voltages of renewable energy is low, the converter will increase the voltage, so that the output voltage is the same as the output voltage of other renewable energy sources. The choke converter method with soft switching produces better performance when compared to conventional choke converters. This converter is capable of optimally sending power to the DC bus. However, this method requires a more complex converter design and setup [16]–[19].

Much previous research has focused on converter design and DC microgrid configurations which has already been widely used. In this paper, a DC microgrid is designed with a hybrid DC/AC coupling configuration. The proposed DC microgrid consisted of two PV arrays, as well as two multi-batteries that could be connected to and disconnected from the utility grid. This design used a 100 Wp PV module and a 200 Ah battery module. The proposed scheme aims to reduce power fluctuations on the DC bus, when the microgrid source of the PV array and battery are disconnected.

II. PV ARRAY

In this study, two PV arrays were used. Each PV array was composed of PV modules and was connected in series and parallel. The capacity of each PV module used was 100 Wp and each PV array was composed of 14 PV modules. A PV module consists of a PV cell, which can be modeled with a diode connected in parallel with a current source, as shown in Figure 1. In this model, two diodes were used to demonstrate the performance of the PV module at low irradiation intensity levels [20]–[22] .

In this PV model, there is a shunt resistance (R_{sh}) which is connected in parallel. A PV cell is described as a current source because the PV cell is a nonlinear component. In the PV model, the value of the R_{sh} is usually very large, while the value of the series resistance (R_s) is very small to reduce the output voltage drop [23], [24]. The current flowing through the R_{sh} can be expressed using (1).

$$I_{sh} = \frac{V+R_s I}{R_{sh}}. \quad (1)$$

While the diode current equation in the PV model is stated in (2).

$$I_D = I_0 \left\{ \exp\left(\frac{V+IR_s}{nN_s V_t}\right) - 1 \right\}. \quad (2)$$

By using the current Kirchoff equation, the output current equation for the PV model is expressed in (3) and (4) [25], [26].

$$I = I_{pv} - I_{D1} - I_{D2} - I_{sh} \quad (3)$$

$$I = I_{pv} - I_{D1} - I_{D2} - \left\{\frac{V+R_s I}{R_{sh}}\right\}. \quad (4)$$

III. DC MICROGRID STRUCTURE

The performance improvement scheme of the proposed DC microgrid is shown in Figure 2. The proposed DC microgrid was a hybrid configuration between DC coupling and AC coupling. In the DC coupling configuration, the PV output was stored on the battery storage and the battery supplied the load. Whereas in the AC coupling configuration, the PV output was connected to the load. Any excess of energies in the PV were stored in the battery storage. Each configuration has advantages and disadvantages, so a hybrid configuration is used to increase the power supply to the load.

The proposed DC microgrid configuration consisted of two PV arrays, a battery, a DC-DC converter, a DC-AC converter, and a load. The PV array was connected to the DC-DC converter with the maximum power point tracking (MPPT) algorithm, functioning to extract the PV output power at the maximum point. Meanwhile, the DC-DC converter connected to the battery was a bidirectional converter that was used to charge and discharge the battery. The DC microgrid was connected to the utility grid via a DC-AC converter. When the microgrid source is cut off due to weather changes for a long time and the battery runs out of energy, the DC-AC converter works as a rectifier. The LC filter was connected to the output of the DC-AC converter which functioned to reduce harmonics due to the converter switching process.

DC microgrid in the new configuration operates autonomously in supplying power to the load. The proposed method can meet the load demand. This depends on the weather or potential intensity of solar irradiation. Based on Figure 2, the relationship between source and load currents can be expressed using (5).

$$i_{PVAA} + i_{PVAB} + i_{B1} + i_{B2} + i_{DCG} + i_{DCB} = 0 \quad (5)$$

where i_{PVAA} is current of PV array A (PVAA), i_{PVAB} is current of PV array B (PVAB), i_{B1} is current of battery 1, i_{B2} is current of battery 2, i_{DCG} is current of utility grid side DC, and i_{DCB} is current of DC load. At the same time, the output power is expressed using (6).

$$P_{PVAA} + P_{PVAB} + P_{B1} + P_{B2} + P_{DCG} + P_{DCB} = 0 \quad (6)$$

where P_{PVAA} is power of PV array A, P_{PVAB} is power of PV array B, P_{B1} is power of battery 1, P_{B2} is power of battery 2, P_{DCG} is power of utility grid, and P_{DCB} is power of load. Negative and positive signs in the equation indicate the process of taking and supplying from the microgrid or into the microgrid.

IV. DC MICROGRID CONTROL

The regulatory scheme plays an important role in regulating the flow of energy in the DC microgrid. It was done by controlling all sources and loads connected to the DC bus. DC microgrid settings were done separately by each converter by sending a reference signal to the converter control. PV operated in MPPT mode with a DC bus voltage reference signal to provide a signal to the voltage controller (VC), then the VC output set the pulse width modulation (PWM) generator to the converter. When the weather as cloudy or when at night, the PV control stopped, and the PV did not provide energy to the DC bus. The battery settings were alternated between battery 1

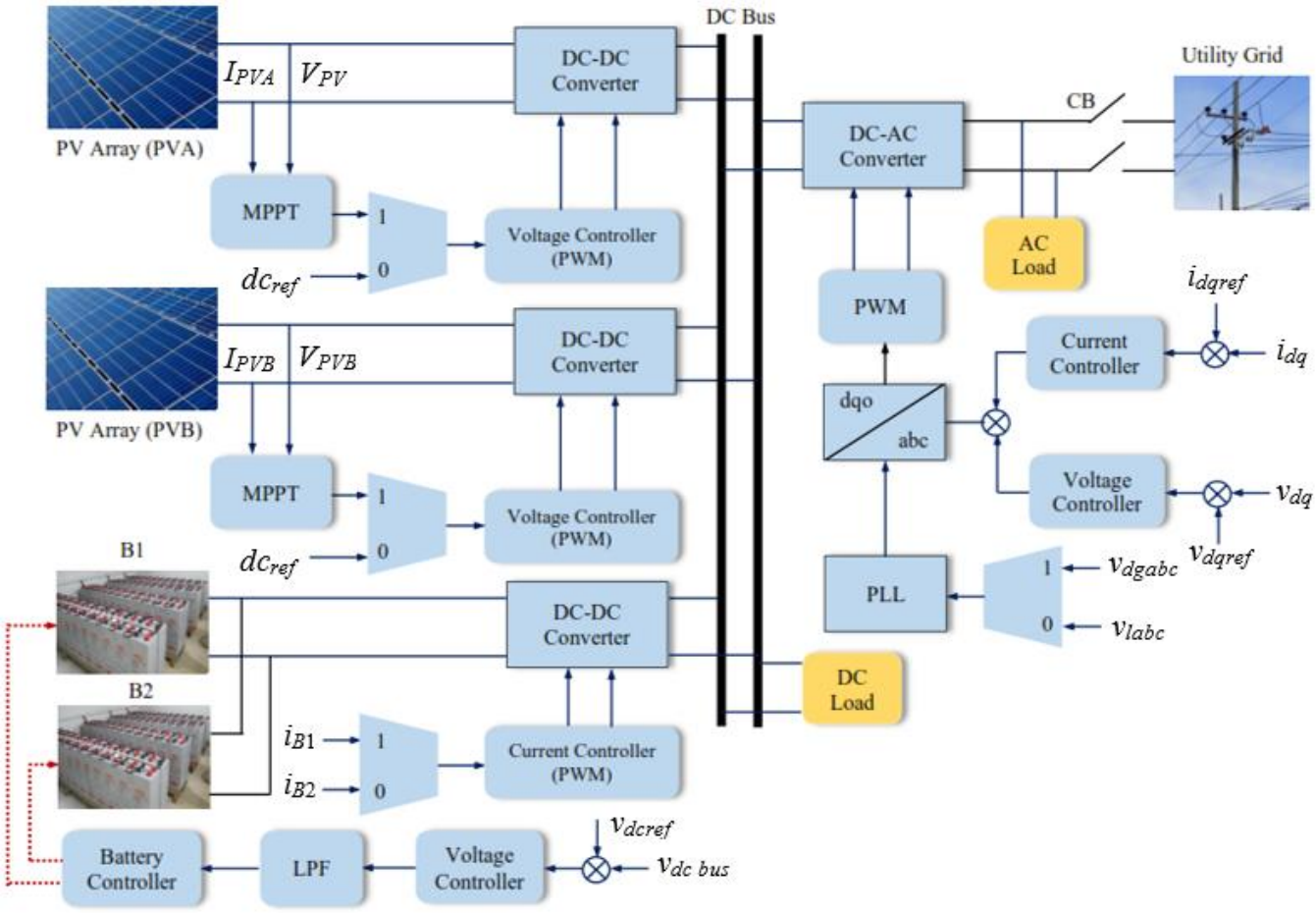

Figure 2. Proposed DC microgrid scheme.

TABLE I
DC MICROGRID PARAMETERS

Component	Parameter	Value
PV array A	Maximum power @ 1000 W/m^2	6 kWp
PV array B	Maximum power @ 1000 W/m^2	4 kWp
Battery 1 and 2	Capacity Voltage Serial connection Parallel connection	@150 Ah @12 V 8 8
DC Bus	Voltage	48 V
Utility grid	Power capacity Voltage, frequency	8 kW 220 V, 50 Hz
Load	DC load AC load	2 kW 1 kW

and battery 2. In battery settings, a voltage sensor was used to determine the stability of the DC bus voltage. This sensor gave a signal to the battery controller (BC) through the low pass filter (LPF) to regulate battery performance. BC regulated the release of battery energy by comparing the voltage of battery 1 and battery 2. When the voltage of battery 1 was greater, battery 1 would operate. Meanwhile, the current controller (CC) set the PWM generator as a signal converter on a DC-AC converter works bidirectional. When the PV source and battery were able to supply the load, the DC-AC converter operated as an inverter and was directly connected to the AC load. In this condition, the circuit breaker (CB) switch/breaker in the utility network was open. The inverter used worked with the phase locked loop (PLL) algorithm. When the PV source and battery were cut off, the CB was closed, and the DC-AC converter operated as a rectifier. In this state, the DC-AC converter supplied the DC source to the DC bus. The process was repeated so that the energy supply to DC loads and AC loads was fulfilled. The research location was carried out in Semarang, while the time for conducting the research was in October 2022.

TABLE II
LOAD DC PARAMETERS

Load Type	Power Rating (W)	Load Capacity (W)
12 LED lamps	18	216
4 outdoor LEDs	200	800
14 CFL laps	30	420
2 40” TVs	97	194
2 DC stoves	185	370

TABLE III
LOAD AC PARAMETERS

Load Type	Power Rating (W)	Load Capacity (W)
1 water pump	300	300
1 washer	340	340
1 freezer box	360	360

Table I shows the PV array, battery, and utility grid source parameters in the DC microgrid system, while Table II and Table III show the various types of DC load and AC load that are used to test the performance of DC microgrid with a hybrid configuration.

V. RESULT AND DISCUSSION

DC microgrid study with a hybrid configuration DC/AC coupling was carried out according to a predetermined location and time. On October 10, 2022, it had a daily solar irradiation intensity of 4,97 kW/m^2. Figure 3 shows the daily solar

JURNAL NASIONAL TEKNIK ELEKTRO DAN TEKNOLOGI INFORMASI
p-ISSN 2301–4156 | e-ISSN 2460–5719

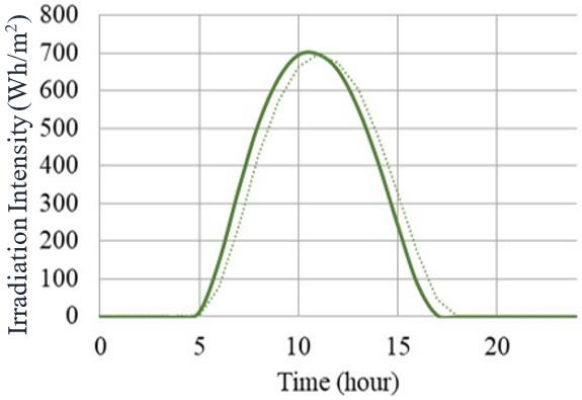

Figure 3. Solar irradiation intensity on 10 October 2022.

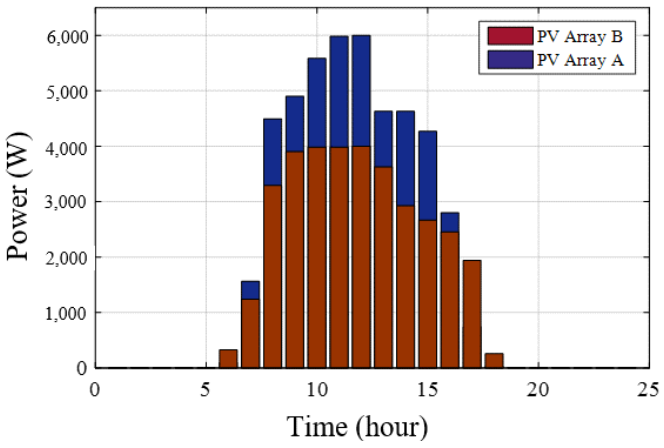

Figure 4. Output power of PV array A and PV array B.

irradiation intensity profile in October 2022. In the profile it can be seen that the peak of solar irradiation intensity occurs at 11.00. Semarang City has the potential to develop microgrids using solar energy.

Semarang had a profile of potential average solar irradiation intensity every month in 2022 which was quite large: January was 131 kWh/m^2, February was 141 kWh/m^2, March was 151 Kwh/m^2, April was 159 Kwh/m^2, May was 158 kWh/m^2, June was 158 kWh /m^2, July was 164 kWh/m^2, August was 171 kWh/m^2, September was 180 kWh/m^2, October was 191 kWh/m^2, November was 161 kWh/m^2, December was 156 kWh/m^2.

A. DC BUS-CONNECTED PV ARRAY

In this study, the microgrid used 6,000 Wp PV Array A (PVAA) and 4,000 Wp PV Array B (PVAB). To test the performance, the system used solar irradiation intensity of 1,000 W/m^2. The MPPT used automatically extracted maximum power from PVAA and PVAB. MPPT operated at 07.00, so PVAA and PVAB provided power for DC loads and AC loads via the DC bus. In addition, some of the PV output power was stored in the battery via a bidirectional DC-DC converter. It can be seen in Figure 4. In the figure it can be seen that PVAA produced maximum output power at 11.00 to 12.00, while PVAB provided maximum output power at 10.00 to 12.00.

The DC microgrid used solar energy for its initial operation, in this case, PVAA and PVAB were connected to the DC bus via a DC-DC converter. During this initial operation, the battery and utility network were not supplying power to the load. The load on this microgrid used a DC load with a capacity of 2 kW and an AC load of 1 kW. Figure 5 shows the profile

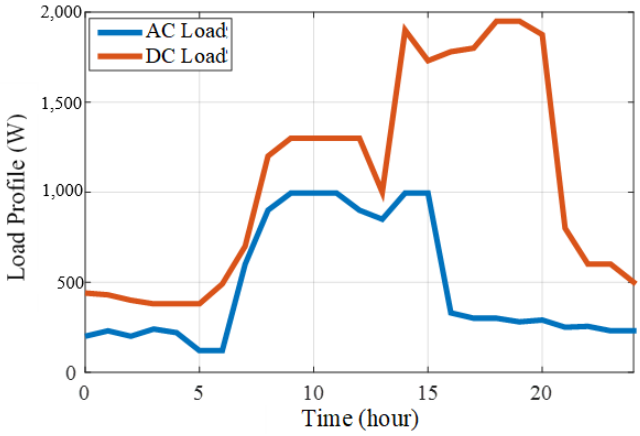

Figure 5. Load profile.

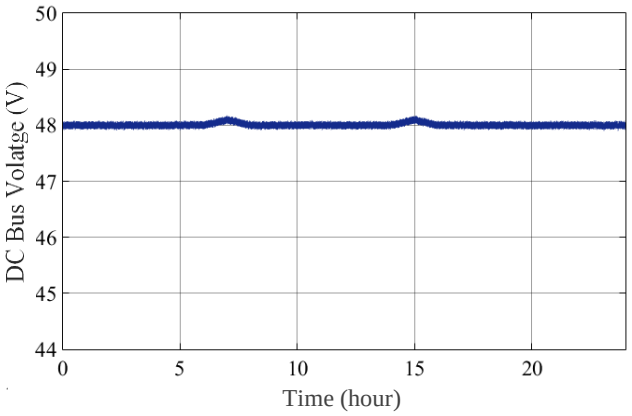

Figure 6. DC bus voltage.

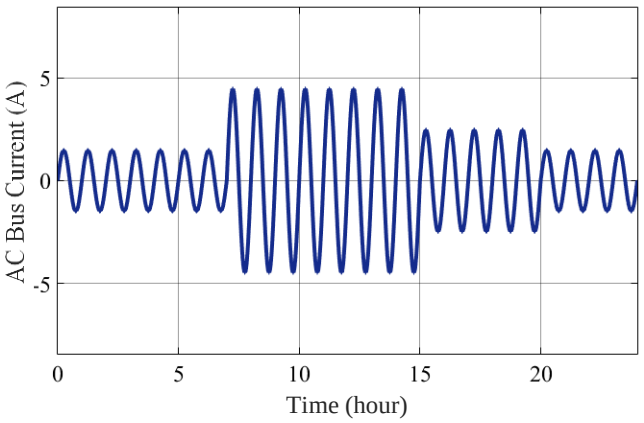

Figure 7. AC load current, PV array source.

on DC load and AC load. When a DC load and an AC load were connected to the DC bus, the DC load increased, from 14.00 to 20.00. Meanwhile, the AC load increased from 08.00 to 15.00.

Figure 6 shows the DC voltage with the source from the PV array. At 08.00 and 15.00 there was a change in the DC bus voltage as a result of a change in the output of the PV array. Figure 7 shows the AC load current. It can be seen from the figure that the maximum current of the AC load at 08.00 to 15.00 was 4.9 A. The lowest load occurred at 20.00 to 08.00. However, with a hybrid configuration, the DC microgrid could stabilize the DC bus voltage at 48 V and could supply the maximum AC load.

B. DC BUS-CONNECTED BATTERY

In the second condition, when there was no solar energy at night or the city of Semarang is cloudy and rainy, the DC

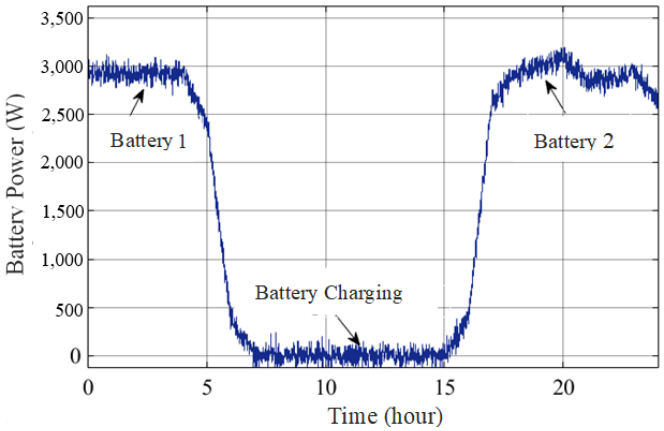

Figure 8. Supply of battery power to the load.

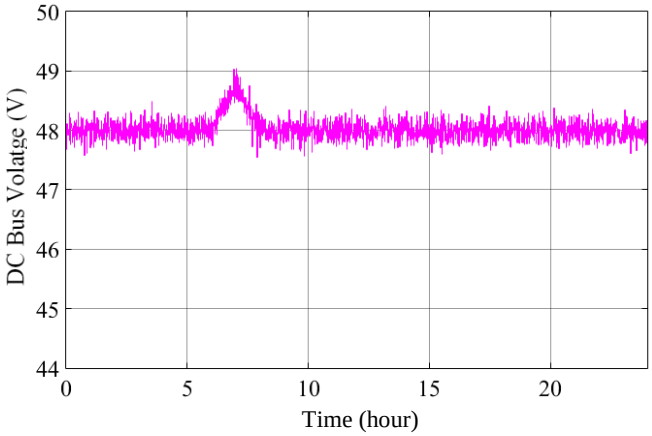

Figure 9. DC bus voltage from the battery source.

microgrid operated in connected mode with the battery storage. In this mode, the energy stored in the battery was used to supply power to the load via the DC bus. In this condition, the output of the PV array was disconnected and did not supply power to the load. Figure 8 shows the change in flow of battery 1 and battery 2 sources to the load. Battery 1 supplied power to the load from 18.00 to 24.00, while battery 2 supplied power to the load from 24.00 to 07.00. The charging process for battery 1 and battery 2 occurred from 07.00 to 18.00.

By using a DC/AC coupling hybrid configuration on the DC microgrid, the voltage changes that occurred at 07.00 could return to stability at 48 V, as shown in Figure 9. In this second condition, battery 1 and battery 2 could supply DC loads and AC loads. In addition, the power supply to the load was not interrupted.

C. DC BUS-CONNECTED UTILITY GRID

The third condition was when the PV source and battery were disconnected and not supplying power to the load. In this condition, the CB connected the utility network source to the DC bus via the AC-DC converter. The load was completely supplied from the utility grid. Figure 10 shows the DC bus voltage spike as a result of a change in load. It can be seen that with the proposed hybrid configuration, the DC bus voltage remained stable at 48 V. The spikes in the DC bus voltage occurred at 07.30, 16.00, and 21.30. Then, Figure 11 shows the network voltage of 220 V and changes in the utility network current. The maximum current from the network to the load occurred at 09.00 to 16.00, while the lowest current occurred at 16.00 to 21.00. In this study, it can be seen that with three conditions or three modes, the DC microgrid was able to supply

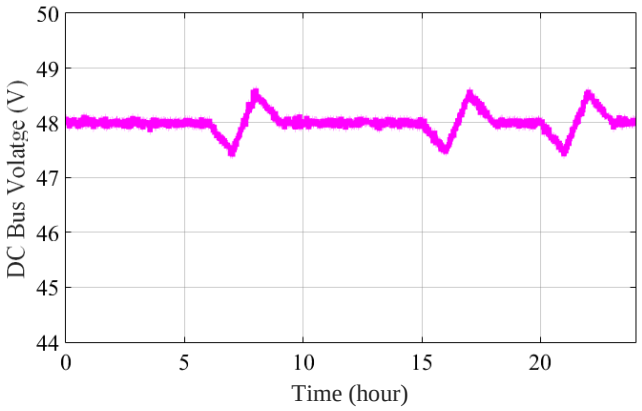

Figure 10. DC bus voltage, utility grid source.

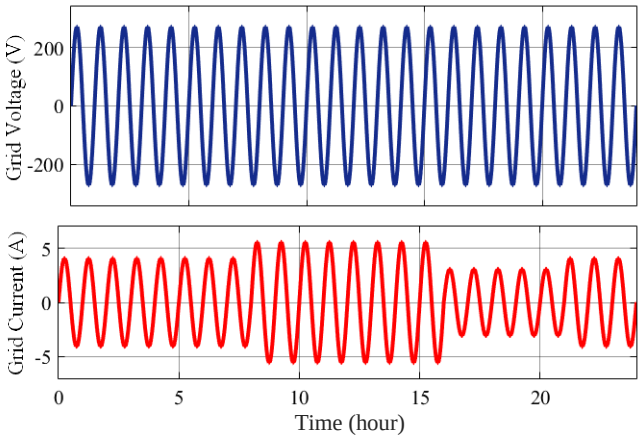

Figure 11. Utility grid voltage and current.

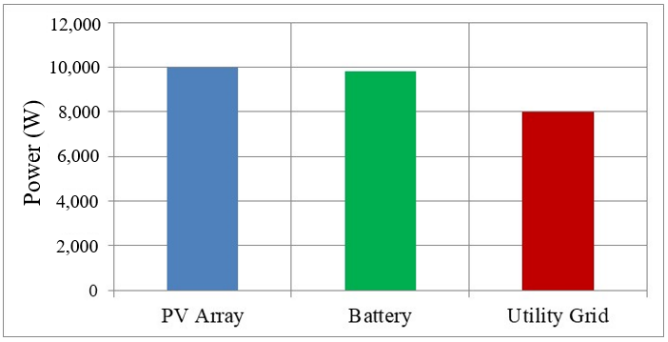

Figure 12. DC microgrid resource capacity.

the load uninterruptedly. Therefore, the DC-AC coupling hybrid configuration on the DC microgrid is able to provide a continuous power source.

Figure 12 shows the power generated from the PV array, battery and utility network, which is shown in the bar graph. It can be seen that the power capacity provided by the DC microgrid was sufficient to meet the demand for DC loads and AC loads.

VI. CONCLUSION

The increased load demand on the DC microgrid was developed with a hybrid DC/AC coupling configuration. The proposed scheme aims to reduce power fluctuations on the DC bus, when the output of the PV array and battery is disconnected. The scheme proposed in this paper is capable of providing stable power and voltage to DC loads and AC loads. It can be seen that the energy capacity stored in the battery affects the supply to the load. The results of the research show

p-ISSN 2301–4156 | e-ISSN 2460–5719

that the voltage spikes on the DC bus could be minimized by using the control scheme for each converter. In addition, the power capacity provided by the DC microgrid was sufficient to meet the demand for DC loads and AC loads. This research focuses on the performance of DC microgrids in meeting load demands. The scheme used in this research can be developed by considering the cost factor and a new control strategy on DC microgrid.

CONFLICT OF INTEREST

The author provides a statement that there is no conflict of interest in this study.

AUTHOR CONTRIBUTION

Conceptualization, Adhi Kusmantoro, and Ardyono Priyadi; methodology, Adhi Kusmantoro, Ardyono Priyadi; software, Adhi Kusmantoro; validation, Adhi Kusmantoro, Ardyono Priyadi; formal analysis, Adhi Kusmantoro; investigation, Adhi Kusmantoro; resources, Ardyono Priyadi; data curation, Adhi Kusmantoro; writing—preparation of the original draft, Adhi Kusmantoro, Ardyono Priyadi; writing—review and editing, Adhi Kusmantoro.

ACKNOWLEDGMENT

We would like to thank LPPM Universitas PGRI Semarang for providing financial support for this research.

REFERENCES

[1] S. Pannala, N. Patari, A.K. Srivastava, and N.P. Padhy, "Effective Control and Management Scheme for Isolated and Grid Connected DC Microgrid," *IEEE Trans. Ind. Appl.*, Vol. 56, No. 6, pp. 6767-6780, Nov.–Des. 2020, doi: 10.1109/TIA.2020.3015819.

[2] Z. Tang, Y. Yang, and F. Blaabjerg, "Power Electronics: The Enabling Technology for Renewable Energy Integration," *CSEE J. Power, Energy Syst.*, Vol. 8, No. 1, pp. 39–52, Jan. 2022, doi: 10.17775/CSEEJPES.2021.02850.

[3] M. Nasir *et al*., "Solar PV-Based Scalable DC Microgrid for Rural Electrification in Developing Regions," *IEEE Trans. Sustain. Energy*, Vol. 9, No. 1, pp. 390–399, Jan. 2018, doi: 10.1109/TSTE.2017.2736160.

[4] S. Abdullahi, T. Jin, and P.M. Lingom, "Robust Control Strategy for Inductive Parametric Uncertainties of DC/DC Converters in Islanded DC Microgrid," *J. Modern Power Syst., Clean Energy*, Vol. 11, No. 1, pp. 335–344, Jan. 2023, doi: 10.35833/MPCE.2021.000241.

[5] S.B.Q. Naqvi and B. Singh, "A PV-Battery System Resilient to Weak Grid Conditions with Regulated Power Injection and Grid Supportive Features," *IEEE Trans. Sustain. Energy*, Vol. 13, No. 3, pp. 1408–1419, Jul. 2022, doi: 10.1109/TSTE.2022.3159110.

[6] A. Suryanto *et al*., "Optimalisasi Keluaran Panel Surya Menggunakan Solar Tracker Berbasis Kamera Terintegrasi Raspberry Pi," *J. Nas. Tek. Elekt., Teknol. Inf.*, Vol. 10, No. 3, pp. 282–290, Aug. 2021, doi: 10.22146/jnteti.v10i3.1142.

[7] H. Silva-Saravia *et al*., "Enabling Utility-Scale Solar PV Plants for Electromechanical Oscillation Damping," *IEEE Trans., Sustain. Energy*, Vol. 12, No. 1, pp. 138–147, Jan. 2021, doi: 10.1109/TSTE.2020.2985999.

[8] R. Bakhshi-Jafarabadi, J. Sadeh, and M. Popov, "Maximum Power Point Tracking Injection Method for Islanding Detection of Grid-Connected Photovoltaic Systems in Microgrid," *IEEE Trans. Power Del.*, Vol. 36, No. 1, pp. 168–179, Feb. 2021, doi: 10.1109/TPWRD.2020.2976739.

[9] A. Affam *et al*., "A Review of Multiple Input DC-DC Converter Topologies Linked with Hybrid Electric Vehicles and Renewable Energy Systems," *Renew. Sustain. Energy Rev.*, Vol. 135, pp. 1–23, Jan. 2021, doi: 10.1016/j.rser.2020.110186.

[10] A.S. Pratiwi, S.D. Nugraha, and E. Sunarno, "Desain dan Simulasi Bidirectional DC-DC Converter untuk Penyimpanan Energi pada Sistem Fotovoltaik," *J. Nas. Tek. Elek., Teknol. Inf.*, Vol. 9, No. 3, pp. 305–310, Aug. 2020, doi: 10.22146/.v9i3.377.

[11] R. Aliaga *et al*., "Implementation of Exact Linearization Technique for Modeling and Control of DC/DC Converters in Rural PV Microgrid Application," *IEEE Access*, Vol. 10, pp. 56925–56936, May 2022, doi: 10.1109/ACCESS.2022.3178425.

[12] W. El Aouni and L.-A. Dessaint, "Real-Time Implementation of Input-State Linearization and Model Predictive Control for Robust Voltage Regulation of a DC-DC Boost Converter," *IEEE Access*, Vol. 8, pp. 192101–192108, Oct. 2020, doi: 10.1109/ACCESS.2020.3032327.

[13] L. Callegaro, M. Ciobotaru, D.J. Pagano, and J.E. Fletcher, "Feedback Linearization Control in Photovoltaic Module Integrated Converters," *IEEE Trans. Power Electron.*, Vol. 34, No. 7, pp. 6876–6889, Jul. 2019, doi: 10.1109/TPEL.2018.2872677.

[14] E.D. Aranda, S.P. Litrán, and M.B.F. Prieto, "Combination of Interleaved Single-Input Multiple-Output DC-DC Converters," *CSEE J. Power, Energy Syst.*, Vol. 8, No. 1, pp. 132–142, Jan. 2022, doi: 10.17775/CSEEJPES.2020.00300.

[15] M. Dhananjaya and S. Pattnaik, "Design and Implementation of a SIMO DC–DC Converter," *IET Power Electron.*, Vol. 12, No. 8, pp. 1868–1879, Jul. 2019, doi: 10.1049/iet-pel.2018.6217.

[16] Z. Sun and S. Bae, "Multiple-Input Soft-Switching DC–DC Converter to Connect Renewable Energy Sources in a DC Microgrid," *IEEE Access*, Vol. 10, pp. 128380–128391, Dec. 2022, doi: 10.1109/ACCESS.2022.3227439.

[17] K.R. Kothapalli *et al*., "Soft-Switched Ultrahigh Gain DC–DC Converter with Voltage Multiplier Cell for DC Microgrid," *IEEE Trans. Ind. Electron.*, Vol. 68, No. 11, pp. 11063–11075, Nov. 2021, doi: 10.1109/TIE.2020.3031453.

[18] S.B. Santra, D. Chatterjee, and Y.P. Siwakoti, "Coupled Inductor Based Soft Switched High Gain Bidirectional DC-DC Converter with Reduced Input Current Ripple," *IEEE Trans. Ind. Electron.*, Vol. 70, No. 2, pp. 1431–1443, Feb. 2023, doi: 10.1109/TIE.2022.3156153.

[19] V. Sidorov, A. Chub, and D. Vinnikov, "High-Efficiency Quad-Mode Parallel PV Power Optimizer for DC Microgrids," *IEEE Trans. Ind. Appl.*, Vol. 59, No. 1, pp. 1002–1012, Jan.–Feb. 2023, doi: 10.1109/TIA.2022.3208879.

[20] M. Kermadi, V.J. Chin, S. Mekhilef, and Z. Salam, "A Fast and Accurate Generalized Analytical Approach for PV Arrays Modeling Under Partial Shading Conditions," *Solar Energy*, Vol. 208, pp. 753–765, Sep. 2020, doi: 10.1016/j.solener.2020.07.077.

[21] R. Abbassi, A. Abbassi, A.A. Heidari, and S. Mirjalili, "An Efficient Salp Swarm-Inspired Algorithm for Parameters Identification of Photovoltaic Cell Models," *Energy Convers., Manage.*, Vol. 179, pp. 362–372, Jan. 2019, doi: 10.1016/j.enconman.2018.10.069.

[22] C. Zhang *et al*., "Modeling and Prediction of PV Module Performance Under Different Operating Conditions Based on Power-Law I–V Model," *IEEE J. Photovolt.*, Vol. 10, No. 6, pp. 1816–1827, Nov. 2020, doi: 10.1109/JPHOTOV.2020.3016607.

[23] A.A.Z. Diab *et al*., "Coyote Optimization Algorithm for Parameters Estimation of Various Models of Solar Cells and PV Modules," *IEEE Access*, Vol. 8, pp. 111102-111140, Jun. 2020, doi: 10.1109/ACCESS.2020.3000770.

[24] D. Yousri *et al*., "Reliable Applied Objective for Identifying Simple and Detailed Photovoltaic Models Using Modern Metaheuristics: Comparative Study," *Energy Convers., Manage.*, Vol. 223, pp. 1–20, Nov. 2020, doi: 10.1016/j.enconman.2020.113279.

[25] D. Yousri *et al*., "Modified Interactive Algorithm Based on Runge Kutta Optimizer for Photovoltaic Modeling: Justification Under Partial Shading and Varied Temperature Conditions," *IEEE Access*, Vol. 10, pp. 20793–20815, Feb. 2022, doi: 10.1109/ACCESS.2022.3152160.

[26] Z. Wu, S. Lv, H. Song, and M. Yun, "Statistical Modeling of UV-Induced PV Module Power Degradation Based on Acceleration Tests," *IEEE J. Photovolt.*, Vol. 10, No. 1, pp. 144–149, Jan. 2020, doi: 10.1109/JPHOTOV.2019.2950590.